



Published in final edited form as:

Int J Radiat Oncol Biol Phys. 2015 November 15; 93(4): 908–915. doi:10.1016/j.ijrobp.2015.08.014.

A radiation-induced hippocampal vascular injury surrogate marker predicts late neurocognitive dysfunction

Reza Farjam^a, Priyanka Pramanik^b, Madhava P. Aryal^b, Ashok Srinivasan^c, Christopher H. Chapman^b, Christina I. Tsien^d, Theodore S. Lawrence^b, and Yue Cao^{b,c,e}

^aDepartment of Medical Physics, Memorial Sloan-Kettering Cancer Center, New York, NY 10065

^bDepartment of Radiation Oncology, University of Michigan, Ann Arbor, MI 48109-5010

^cDepartment of Radiology, University of Michigan, Ann Arbor, MI 48109-5842

^dDepartment of Radiation Oncology, Washington University in St. Louis, St. Louis, MO, 63110

^eDepartment of Biomedical Engineering, University of Michigan, Ann Arbor, MI 48109-2099

Abstract

Purpose—We aimed to develop a hippocampal vascular injury surrogate marker for early prediction of late neurocognitive dysfunction in patients receiving brain radiotherapy (RT).

Methods and Materials—27 patients (17 males and 10 females, age 31–80 years) were enrolled in an IRB-approved prospective longitudinal study. Patients were diagnosed with a low-grade glioma or benign tumor and treated by 3-D conformal or intensity-modulated RT with a median dose of 54 Gy (50.4–59.4 Gy in 1.8-Gy fractions). Six dynamic-contrast enhanced MRI scans were performed from pre-RT to 18-month post-RT, and quantified for vascular parameters related to blood-brain barrier permeability, K^{trans} , and the fraction of blood plasma volume, V_p . The temporal changes in the means of hippocampal K^{trans} and V_p after starting RT were modeled by integrating the dose effects with age, sex, hippocampal laterality and presence of tumor/edema near a hippocampus. Finally, the early vascular dose-response in hippocampi was correlated with neurocognitive dysfunction 6 and 18-months post-RT.

Results—The K^{trans} mean increased significantly from pre-RT to 1-month post-RT ($p < 0.0004$), which significantly depended on sex ($p < 0.0007$) and age ($p < 0.00004$), with the dose-response more pronounced in older females. Also, the vascular dose-response in the left hippocampus of females correlated significantly with changes in memory function at 6 ($r = -0.95$, $p < 0.0006$) and 18-months ($r = -0.88$, $p < 0.02$) post-RT.

Corresponding author: Yue Cao, Ph.D., Department of Radiation Oncology, University of Michigan, 519 W William St, Ann Arbor, MI 48103, Phone: (734)647-2914, Fax: (734)936-7859, yuecao@umich.edu.

None of the authors has any conflict of interest regarding this work.

Publisher's Disclaimer: This is a PDF file of an unedited manuscript that has been accepted for publication. As a service to our customers we are providing this early version of the manuscript. The manuscript will undergo copyediting, typesetting, and review of the resulting proof before it is published in its final citable form. Please note that during the production process errors may be discovered which could affect the content, and all legal disclaimers that apply to the journal pertain.

Conclusions—The early hippocampal vascular dose-response could be a predictor of late neurocognitive dysfunction. A personalized hippocampus sparing strategy may be considered in the future.

Keywords

Hippocampal Sparing; Radiation-Induced Neurocognitive Dysfunction; And Multivariate Interaction Model

Introduction

Radiation-induced injury to the central nervous system and neurocognitive dysfunction are severe complications in long-term brain tumor survivors receiving radiotherapy (RT). Clinical complications of RT include acute, delayed and late-delayed injury¹. Acute injury, occurring hours to weeks after irradiation, may result from radiation-induced cerebral edema^{2, 3}, while delayed injury, happening 1–6 months after irradiation, is thought partially due to transient interruption of myelin synthesis secondary to oligodendrocyte injury. Both acute and delayed injuries may be reversible and recover spontaneously^{5, 6}. In contrast, the late-delayed effects, observed more than 6 months after irradiation, are thought to be irreversible and progressive. The most severe symptoms are formation of radiation-induced necrosis and progressive cognitive deterioration^{4, 7}. The latter can occur without tissue necrosis or anatomic abnormality.

The exact mechanism of radiation-induced learning and memory declines in brain tumor survivors is unclear. However, it could relate to limbic system as well as hippocampus malfunctioning⁸. The hippocampus is believed to be responsible for the formation of verbal memory, so its dysfunction could decrease patient ability to consolidate short-term memory to long-term memory⁹. Radiation can induce vascular injury¹⁰ that may lead to hippocampus impairment. Considering limited treatment options for cognitive dysfunction, strategies for preventing detrimental cognitive effects after brain RT have been explored in RTOG clinical trials (0933 and 0614) of whole brain RT (WBRT) for brain metastases. One trial explores the hypothesis that sparing the hippocampus during WBRT preserves memory function¹¹, and another tests a vascular dementia drug (memantine) for preventing cognitive declines after RT¹². However, insufficient attention is given to the patients who are long-term survivors and received partial brain RT. Studying the hippocampal vascular response to radiation in this patient population and relating it to late-delayed memory function changes could provide critical dosimetric evidence to guide organ-at-risk sparing and/or drug intervention for preserving memory function in the patients. Also, the hippocampal dose-variation in the population provides an opportunity to evaluate dose effects, which is impossible in the patients receiving WBRT.

In this study, we investigated radiation-induced alterations in hippocampal vascular properties as a hippocampal injury surrogate marker for the delayed and late-delayed neurocognitive declines in patients treated by partial brain RT. We assessed radiation-induced longitudinal changes in hippocampal vasculature from pre-RT to 18 months post-RT, and the influence of clinical factors of sex, age, and edema on dose effects. To this end,

we used the dynamic contrast enhanced (DCE)-MRI to characterize changes in vascular permeability and microvessel dilation or shrinkage as an indicator of vascular injury, and correlated their changes with delayed and late-delayed neurocognitive declines.

Materials and Methods

Patients

Between August 2004 and January 2012, 27 patients (17 men and 10 women, and the age range of 31–80 years) were enrolled in an institutional review board (IRB)-approved prospective longitudinal study (Table 1). The patients were treated by three-dimensional conformal or intensity-modulated RT, with a median dose of 54 Gy (range of 50.4–59.4 Gy in 1.8-Gy fractions), for low-grade glioma, grade 3 anaplastic ependymoma, meningioma, craniopharyngioma, or pituitary adenoma. None of these patients received chemotherapy during RT. Patients underwent MRI scans prior to RT (Pre-RT), 3 weeks after starting RT (Mid-RT), at the end of RT (End-RT), and 1 month (1M), 6 months (6M) and 18 months (18M) after completion of RT. Also, patients underwent a battery of standardized neurocognitive tests Pre-RT, and at 1M, 6M, and 18M post-RT. One patient (#13) continuously received hydrocortisone from Pre-RT up to 6M post-RT, and one other (#17) received dexamethasone during and until the end of RT. Of the 27 patients, one patient did not have the DCE-MRI data Mid-RT, 1 at End-RT, 4 at 1M post-RT, and 3 at 6M post-RT. Also, five patients did not have neurocognitive tests at 18M follow-up. So, the missing data were not available for analysis.

MRI acquisition

MRI scans at each time included pre- and post-Gd-DTPA volumetric T1-weighted, T2-weighted fluid-attenuated inversion recovery (FLAIR), and 3-D volumetric DCE T1-weighted images. To eliminate the time-of-flight effect from in-flow blood proton spins, all DCE images were acquired in the sagittal plane and covered the whole brain. For the first 12 patients who were scanned on a 1.5-T system (General Electric HealthCare), the DCE images were acquired using a 3-D gradient echo sequence with a flip angle of 20°, TE/TR of 1.08/3.4 ms, a voxel size of $0.86 \times 0.86 \times 6 \text{ mm}^3$ and a temporal resolution of approximately 6 seconds. Due to the system upgrade, the remaining 15 patients had scans on a 3-T scanner (Philips Healthcare), and had the DCE images acquired with TE/TR of 1.05/5.14 ms, a voxel size of $2 \times 2 \times 2 \text{ mm}^3$. All patients had a single dose (0.1 mL/kg) of Gd-DTPA, injected at a rate of 2 mL/s. No patient was scanned on different scanners.

Neurocognitive tests

The neurocognitive tests included the Controlled Oral Word Association (COWA) test¹³, the revised Hopkins Verbal Learning Test (HVLT-R)¹⁴, and Trail Making Tests (TMT) A and B¹⁵. HVLT-R assesses verbal memory (recall and delayed recall) and learning component. The TMTA assesses attention and information processing efficiency. TMTB is used for mental flexibility and executive function. COWA assesses word fluency and executive function. These tests are well established in patients receiving RT¹⁶ and have been used in several RTOG trials, e.g., RTOG 0212, RTOG 0614 and RTOG 0933. The standardized Z-

scores from all test scores were calculated to adjust age, sex, and education effects on raw scores accordingly^{14, 17, 18}.

Image registration

All images, including anatomic MRI, DCE-MRI and treatment planning CT, were co-registered using a mutual information and simplex optimization algorithm from an in-house software package (FIAT)^{19–20}. Initially, the DCE images were co-registered within the series to correct any possible misalignment prior to kinetic variable estimation. At each time point, the high-resolution post-Gd T1-weighted images were registered to the DCE images, and other images were registered to the registered post-Gd T1-weighted images. Finally, the planned 3-D dose distribution maps were registered to the post-Gd T1-weighted images Pre-RT.

Hippocampus contouring

All hippocampi were manually contoured on the post-Gd-DTPA T1-weighted images according to the hippocampus contouring guidance developed for RTOG 0933. Both hippocampi of a patient were visually examined on T1-weighted and FLAIR MRI to make sure they are not adjacent to or affected by the tumor or edema. Nineteen of 27 patients (either benign or low-grade Glioma) had both intact hippocampi visually (Table 1), and were selected for assessment of radiation-induced neurocognitive dysfunction.

Estimation of kinetic variables from DCE-MRI

The modified Toft model²¹ was used to estimate the kinetic parameters including the transfer constant (K^{trans}) of gadolinium influx from the intravascular space into the extravascular extracellular space and the fractional plasma volume (V_p) in tissue. An increase in K^{trans} is an indicator of vascular leakiness (blood-brain barrier (BBB) permeability to gadolinium-DTPA), and changes in V_p could be related to vaso-constriction or dilation. The arterial input function was obtained from carotid arteries. Note that V_p obtained by this model was corrected for vascular leakage. For each hippocampal structure, we computed the mean (M) and standard deviation (STD) of V_p and K^{trans} .

Statistical analysis

We focused on the dose-dependent changes in V_p and K^{trans} of the hippocampal structures from pre-RT (baseline) to 1 month post-RT for prediction of the delayed (6M) and late-delayed (18M) neurocognitive dysfunction.

Dose effect on the temporal changes of vascular properties—The dose-effects on the mean V_p or K^{trans} of a hippocampus were modeled by a linear regression. In the model, we considered dose interactions with co-variables, such as age, sex, left vs. right hippocampus, and edema as the disease effect as:

$$\Delta\mu(V_p \text{ or } K^{\text{trans}})_{\text{pre-RT} \rightarrow \tau} = \gamma_0 + \text{Dose} \times [\gamma_1 \times \text{Sex} + \gamma_2 \times \text{Age} + \gamma_3 \times \text{LRH} + \gamma_4 \times \text{Edema}] \quad (1)$$

where τ represents the time after starting RT, *Sex* indicates male vs. female, *Age* is a continuous variable in year, *LRH* denotes left vs. right hippocampus, and *Edema* marks as 1

if a hippocampus is near edema and 0 otherwise. Also, *Dose* is the mean radiation dose in each hippocampus, in which the fraction-size variation was corrected to 2-Gy equivalent by the linear-quadratic equation with $\alpha/\beta = 2.5 \text{ Gy}^{22}$. To control the false discovery rate in multiple regressions, a Bonferroni-type sequential procedure²³ was performed, in which a regression was considered statistically significant when $p_1 < \alpha_i$ where p_1 is the i^{th} smallest p -value from m regressions and $\alpha_i = 0.05 * i/m$. In our study, we had 2 kinetic variables (V_p and K^{trans}) and 3 time points (Pre-RT to Mid-RT, End-RT, and 1 month post-RT), resulting in $m = 6$. We also tested whether the scanner type affected the results by including a regressor in Eq. [1], and then found the scanner type was not significant.

Correlation with delayed and late-delayed neurocognitive changes—We assessed whether the radiation-induced changes in vascular properties of either left or right hippocampus could predict the delayed and late-delayed neurocognitive decline. Hence, correlations between the early changes in the hippocampal means of K^{trans} or V_p up to 1 month after RT and the delayed and late-delayed changes (6M and 18M after RT) in the standardized age- and education-adjusted Z-scores of neurocognitive functions were tested by Pearson correlation. To avoid the confounding effect of tumor/edema on analysis, we only considered the patients who had both hippocampi intact. Also, the patient with grade 3 Ependymoma was also excluded from the analysis and only benign tumors were considered.

Post-hoc analysis—For the significant clinical variables in Eq (1), we further investigated if there were any significant differences of the temporal changes in the mean hippocampal V_p or K^{trans} between the subgroups using the paired t -test. Also, we performed the non-parametric Mann-Whitney U Test to investigate whether delayed and late-delayed neurocognitive declines were significantly different between males and females. The p values < 0.05 were considered significant.

Results

Clinical and radiological findings

Up to 18 months after the completion of RT, none of the patients showed tumor progression and radiation-induced lesions on T2-weighted FLAIR and post-Gd T1-weighted images. In all glioma patients, increased signal intensities on FLAIR images in the tumor and its vicinity prior to RT were stable or decreased during the 18-month follow-up. Also, no additional areas of radiation-induced abnormalities on the conventional MRI were present during follow-up. In patients with pituitary adenomas and craniopharyngioma, no signal abnormality outside the tumor was present pre-treatment and no interval change was seen during the 18-month follow-up. In the patient with meningioma, no changes on FLAIR signals beyond the surgical cavity were seen over follow-ups.

Dose effect on the temporal changes of vascular properties

The multivariate linear regression model revealed that changes in the hippocampal K^{trans} from pre-RT to 1M post-RT was significantly predicted ($p < 0.0004$) by the interactions of Dose and Sex ($\gamma_1 = 1.11 \times 10^{-3}$, $p = 0.0007$), Dose and Age ($\gamma_2 = 0.005 \times 10^{-3}$, $p = 0.00004$), and Dose and Edema near the hippocampus ($\gamma_4 = -1.1 \times 10^{-3}$, $p = 0.014$). *Post-*

hoc analysis further illustrated these effects, as (1) a higher radiation dose (> 19 Gy, the median hippocampal dose for all patients included in this study) induced a greater K^{trans} change in female hippocampi ($K^{\text{trans}} = 0.007 \pm 0.0038 \text{ min}^{-1}$, $p = 0.04$) than in male hippocampi (Fig 1(A)); (2) a high dose affects older patients (>50 years, the median age of patients) ($K^{\text{trans}} = 0.004 \pm 0.0024 \text{ min}^{-1}$, $p = 0.04$) greater than younger patients (Fig 1(B)); and (3) the K^{trans} change was more pronounced in old females ($K^{\text{trans}} = 0.005 \pm 0.003 \text{ min}^{-1}$, $p = 0.05$). Furthermore, the edema interaction with dose indicated that the edema-affected hippocampus had a lesser extent change in the K^{trans} than the normal hippocampus receiving the same dose. However, there were no significant differences in radiation dose to the left and right hippocampi ($p = 0.54$) and the dose effect on the K^{trans} changes between left and right hippocampi ($p = 0.5$).

The time profile changes in the mean K^{trans} of females and males are shown in Fig 2. Fig. 2(A) shows that the mean K^{trans} in female hippocampi reached a maximum 1M post-RT and then were subsided 6M and 18M post-RT. In contrast, Fig 2(B) reveals that the mean K^{trans} changes in male hippocampi are significantly less than in female, even though male hippocampi received significantly higher doses ($27.3 \pm 16.7 \text{ Gy}$) than female hippocampi ($18.5 \pm 16.3 \text{ Gy}$), $p = 0.04$.

Finally, Fig. 3 shows an example of the K^{trans} maps within the hippocampal contours (Yellow) pre-RT and 1M post-RT, and related planning isodose curves. Pre-RT, only a few voxels had a K^{trans} value greater than zero (colored voxels). However, more voxels had non-zero K^{trans} value 1M post-RT, indicating an increase in BBB permeability. Finally, we observed no significant dose effect on temporal changes in fractional plasma volume, V_p .

Correlation with delayed and late-delayed neurocognitive changes

The analysis of the neurocognitive test scores in patients with intact hippocampi (as described above) showed delayed-recall Z-scores of the HVLt-R test in females gradually decreased from $Z = 0.31 \pm 0.23$ (SEM) pre-RT to $Z = -0.66 \pm 0.27$ 18M post-RT, which was significant with $p < 0.05$ (Fig 4). Previous data^{14, 17} have shown the average test-retest variability of Z-scores of the neurocognitive tests approximately ± 0.25 , and indicated a decline of >0.5 clinically significant. Hence, a Z-score decline of -0.97 (from 0.31 to -0.66) in the delayed-recall test of females indicated a clinically significant decline in memory function. No such trends were observed for men or other neurocognitive test scores.

Most importantly, the changes in the mean K^{trans} of the female left hippocampi from Pre-RT to 1M Post-RT were significantly correlated with changes in the delayed recall Z-scores of the HVLt-R 6M ($r = -0.95$, $p = 0.0006$) and 18M ($r = -0.88$, $p = 0.019$) post-RT. However, such correlations between the early K^{trans} changes in the female right hippocampi and changes in the delayed-recall Z-scores 6M ($r = -0.76$, $p = 0.04$) and 18M ($r = -0.37$, $p = 0.46$) post-RT were much weaker and only significant at 6 month. However, we observed no such trend in males.

Discussion

In this paper, we developed a multivariate regression model to evaluate the hippocampal vascular dose-response as a potential surrogate marker for hippocampal dysfunction in the patients treated by partial brain RT. We investigated the dose effect on the blood-brain barrier permeability as well as the dose interactions with clinical factors, such as sex, age and edema. We observed that radiation induced BBB opening in hippocampi one month after completion of radiotherapy depending on the patient age and sex, with the dose-response more pronounced in older females. Most importantly, the early BBB opening in the female hippocampus was correlated with the delayed and late-delayed memory function declines. The greater sensitivity to radiation-induced neurocognitive declines in the elderly females is supported by the biological findings of radiation-caused aging-like pathology²⁶.

Quantitative imaging allows us to study individual radiation sensitivity and analyze dose-responses in various subgroups systematically. In this study, we found that the radiation-induced hippocampal vascular injury and the subsequent neurocognitive decline are age- and sex- dependent. Although the exact mechanism of the age-dependent radiosensitivity remained unknown, previous studies^{24, 25} have shown that RT has more adverse effects on older patients. Moreover, the radiation-induced aging-like pathology in cerebrocortical cells has been suggested²⁶, including shrinkage of cortical thickness, activation of cell-cycle arrest pathway and inhibition of DNA double strand break repair. Also, it has been shown that exposing cerebral cortex to radiation increases chronic oxidative stress, oxidant DNA damage, lipid peroxidation, and apoptosis²⁶. In terms of sex-dependent radiation sensitivity, higher mortality and morbidity rates from radiation-induced injury in females have been reported²⁷; also, it has been shown that girls could be more sensitive than boys in learning and memory decline following conformal radiotherapy²⁸. However, the sex-dependency of the radiation-induced neurocognitive impairments has not been extensively studied, and needs to be interpreted cautiously. As noted, the patient number in this study is small. Most females underwent MR scans on the Philips scanner in our study. Whether the sex-dependency of the K^{trans} change is due to variations in image acquisitions and magnet field strength was tested and found to be not significant. Also, no patient showed radiation-induced anatomic abnormality or tumor progression, the latter is unlikely a factor affecting our findings. Nonetheless, further verification of the results is needed using a larger dataset and standard imaging protocol. Also, to figure out why females are more sensitive to radiation than males could be the subject of radiobiology studies.

The findings of this study support personalized hippocampal sparing in patients receiving brain radiotherapy²⁹ in a way that the patient's sex and age may need to be considered in the treatment plan for preventing memory function. Indeed, due to short survival time, hippocampal sparing, although helpful, may be less significant in patients with brain metastases in contrast to mitigation of the disease symptoms. However, it would be extremely important in the patients who have low-grade glioma or benign brain tumor and are long-term survivors. In this study, we found that exposing hippocampus to a mean dose of 19-Gy (2-Gy equivalent) or less seemed to result in little or no memory function decline or vascular injury, which could be considered in the dosimetry guidance in a future study. Nonetheless, neurogenesis in the hippocampal subgranular zone has very high sensitivity to

radiation doses^{30–32} where even a low dose at 2-Gy can decrease the production of new neurons and proliferating cells dramatically. Also, changes in neurogenesis have been associated with a significant inflammatory response as indicated by activation of microglia^{30–32}. Based upon animal studies, it has been hypothesized that hippocampal neurogenesis damage is responsible for neurocognitive declines³³. Hence, more studies are needed to further gain our understanding in the relationship between hippocampal dosimetry, neurogenesis, and neurocognitive dysfunction.

In this study, we focused on radiosensitivity of the hippocampal vasculature and its association with hippocampus dysfunction. Vasculatures of the hippocampus, an important structure for memory and learning function, are sensitive to radiation, and seem to be more for older females. Earlier vascular alterations are translated into late neurocognitive function declines. Considering brain functioning as a network, a future study that incorporates radiation effects on hippocampus with interconnecting white matter tracts, frontal lobe components, and clinical factors^{34–37} could lead to an even better prediction for late cognitive dysfunction.

Acknowledgments

This work is supported in part by NIH grants RO1 NS064973.

References

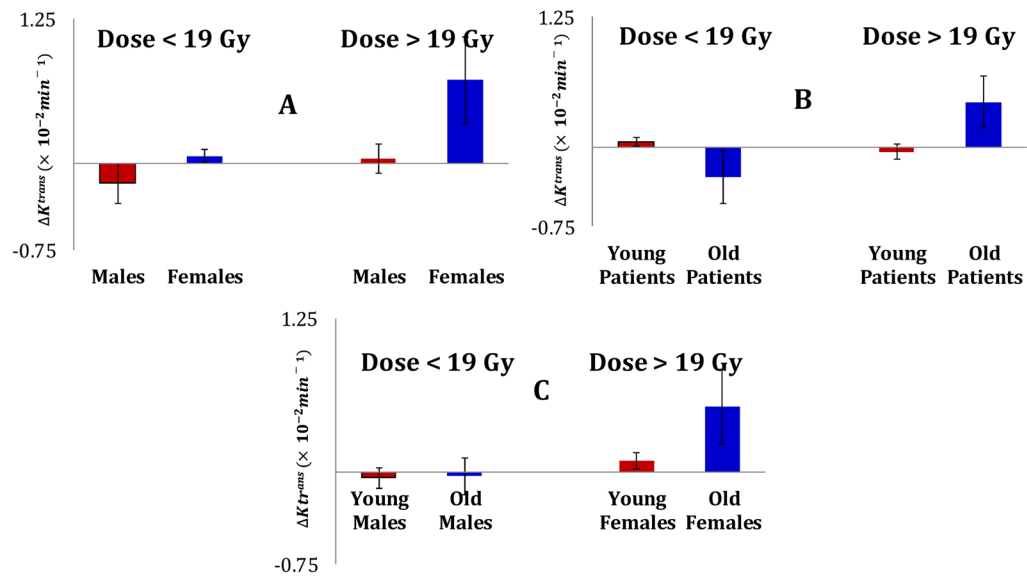
1. Fink J, Born D, Chamberlain MC. Radiation necrosis: relevance with respect to treatment of primary and secondary brain tumors. *Curr Neurol Neurosci Rep.* 2012; 12(3):276–85. [PubMed: 22350279]
2. Young DF, Posner JB, Chu F, Nisce L. Rapid-course radiation therapy of cerebral metastases: results and complications. *Cancer.* 1974; 34(4):1069–76. [PubMed: 4418812]
3. Hindo WA, DeTrana FA 3rd, Lee MS, Hendrickson FR. Large dose increment irradiation in treatment of cerebral metastases. *Cancer.* 1970; 26(1):138–41. [PubMed: 5424525]
4. Armstrong CL, Shera DM, Lustig RA, Phillips PC. Phase measurement of cognitive impairment specific to radiotherapy. *International journal of radiation oncology, biology, physics.* 2012; 83(3):e319–24.
5. Rider WD. Radiation damage to the brain--a new syndrome. *Journal of the Canadian Association of Radiologists.* 1963; 14:67–9. [PubMed: 13982232]
6. Hoffman WF, Levin VA, Wilson CB. Evaluation of malignant glioma patients during the postirradiation period. *J Neurosurg.* 1979; 50(5):624–8. [PubMed: 430157]
7. Kumar AJ, Leeds NE, Fuller GN, et al. Malignant gliomas: MR imaging spectrum of radiation therapy- and chemotherapy-induced necrosis of the brain after treatment. *Radiology.* 2000; 217(2): 377–84. [PubMed: 11058631]
8. Gondi V, Hermann BP, Mehta MP, Tome WA. Hippocampal dosimetry predicts neurocognitive function impairment after fractionated stereotactic radiotherapy for benign or low-grade adult brain tumors. *International journal of radiation oncology, biology, physics.* 2013; 85(2):348–54.
9. Squire LR. Memory and the hippocampus: a synthesis from findings with rats, monkey, and humans. *Psychol Rev.* 1992; 99:195–231. [PubMed: 1594723]
10. Monje ML, Palmer T. Radiation injury and neurogenesis. *Current opinion in neurology.* 2003; 16(2):129–34. [PubMed: 12644738]
11. Gondi, V.; Mehta, MP.; Pugh, S., et al. Memory preservation with conformal avoidance of the hippocampus during whole-brain radiotherapy (WBRT) for patients with brain metastases: Primary endpoint results of RTOG 0933. *ASTRO annual meeting; 2013;*

12. Brown PD, Pugh S, Laack NN, et al. Memantine for the prevention of cognitive dysfunction in patients receiving whole-brain radiotherapy: a randomized, double-blind, placebo-controlled trial. *Neuro-oncology*. 2013; 15(10):1429–37. [PubMed: 23956241]
13. Benton, AL.; Hamsher, Kd; Sivan, AB. *Multilingual Aphasia Examination*. 3. Iowa City, IA: AJA Associates; 1994.
14. Benedict RHB, Schretlen D, Groninger L, Brandt J. Hopkins Verbal Learning Test – Revised: Normative Data and Analysis of Inter-Form and Test-Retest Reliability. *The Clinical Neuropsychologist*. 1998; 12(1):43–55.
15. Bowie CR, Harvey PD. Administration and interpretation of the Trail Making Test. *Nature protocols*. 2006; 1(5):2277–81. [PubMed: 17406468]
16. Mehta MP, Shapiro WR, Glantz MJ, et al. Lead-in phase to randomized trial of motexafin gadolinium and whole-brain radiation for patients with brain metastases: centralized assessment of magnetic resonance imaging, neurocognitive, and neurologic end points. *Journal of clinical oncology: official journal of the American Society of Clinical Oncology*. 2002; 20(16):3445–53. [PubMed: 12177105]
17. Ruff RM, Light RH, Parker SB, Levin HS. Benton Controlled Oral Word Association Test: reliability and updated norms. *Archives of clinical neuropsychology: the official journal of the National Academy of Neuropsychologists*. 1996; 11(4):329–38. [PubMed: 14588937]
18. Tombaugh TN. Trail Making Test A and B: normative data stratified by age and education. *Archives of clinical neuropsychology: the official journal of the National Academy of Neuropsychologists*. 2004; 19(2):203–14. [PubMed: 15010086]
19. Meyer CR, Boes JL, Kim B, et al. Demonstration of accuracy and clinical versatility of mutual information for automatic multimodality image fusion using affine and thin-plate spline warped geometric deformations. *Medical image analysis*. 1997; 1(3):195–206. [PubMed: 9873906]
20. Cao Y. Development of Image Software Tools for Radiation Therapy Assessment. *Medical Physics*. 2005; 32(6):2136.
21. Tofts PS, Brix G, Buckley DL, et al. Estimating kinetic parameters from dynamic contrast-enhanced T(1)-weighted MRI of a diffusible tracer: standardized quantities and symbols. *Journal of magnetic resonance imaging: JMIR*. 1999; 10(3):223–32. [PubMed: 10508281]
22. Barton M. Tables of equivalent dose in 2 Gy fractions: a simple application of the linear quadratic formula. *International journal of radiation oncology, biology, physics*. 1995; 31(2):371–8.
23. Benjamini Y, Hochberg Y. Controlling the False Discovery Rate - a Practical and Powerful Approach to Multiple Testing. *J Roy Stat Soc B Met*. 1995; 57(1):289–300.
24. Douw L, Klein M, Fagel SS, et al. Cognitive and radiological effects of radiotherapy in patients with low-grade glioma: long-term follow-up. *Lancet neurology*. 2009; 8(9):810–8. [PubMed: 19665931]
25. Tabouret E, Tassy L, Chinot O, Cretel E, Retornaz F, Rousseau F. High-grade glioma in elderly patients: can the oncogeriatrician help? *Clinical interventions in aging*. 2013; 8:1617–24. [PubMed: 24353408]
26. Suman S, Rodriguez OC, Winters TA, Fornace AJ Jr, Albanese C, Datta K. Therapeutic and space radiation exposure of mouse brain causes impaired DNA repair response and premature senescence by chronic oxidant production. *Aging*. 2013; 5(8):607–22. [PubMed: 23928451]
27. National Research Council (U.S.). *Health risks from exposure to low levels of ionizing radiation: BEIR VII Phase 2*. Washington, D.C: National Academies Press; 2006. Committee to Assess Health Risks from Exposure to Low Level of Ionizing Radiation.
28. Di Pinto M, Conklin HM, Li C, Merchant TE. Learnin and memory following conformal radiation therapy for pediatric craniopharyngioma and low-grade glioma. *International journal of radiation oncology, biology, physics*. 2012; 84(3):363–9.
29. Gutierrez AN, Westerly DC, Tome WA, et al. Whole brain radiotherapy with hippocampal avoidance and simultaneously integrated brain metastases boost: a planning study. *International journal of radiation oncology, biology, physics*. 2007; 69(2):589–97.
30. Ferrer I, Serrano T, Alcantara S, Tortosa A, Graus F. X-ray-induced cell death in the developing hippocampal complex involves neurons and requires protein synthesis. *Journal of neuropathology and experimental neurology*. 1993; 52(4):370–8. [PubMed: 8355026]

31. Mizumatsu S, Monje ML, Morhardt DR, Rola R, Palmer TD, Fike JR. Extreme sensitivity of adult neurogenesis to low doses of X-irradiation. *Cancer research*. 2003; 63(14):4021–7. [PubMed: 12874001]
32. Nagai R, Tsunoda S, Hori Y, Asada H. Selective vulnerability to radiation in the hippocampal dentate granule cells. *Surgical neurology*. 2000; 53(5):503–6. discussion 6–7. [PubMed: 10874152]
33. Greene-Schloesser D, Moore E, Robbins ME. Molecular pathways: radiation-induced cognitive impairment. *Clinical cancer research: an official journal of the American Association for Cancer Research*. 2013; 19(9):2294–300. [PubMed: 23388505]
34. Hau C, Merchant TE, Gajjar A, et al. Brain tumor therapy-induced changes in normal-appearing brainstem measured with longitudinal diffusion tensor imaging. *International journal of radiation oncology, biology, physics*. 2012; 82(5):2047–54.
35. Uh J, Merchant TE, Li Y, et al. Differences in brainstem fiber tract response to radiation: a longitudinal diffusion tensor imaging study. *International journal of radiation oncology, biology, physics*. 2012; 86(2):292–7.
36. Chapman CH, Nazem-Zadeh M, Lee OE, et al. Regional variation in brain white matter diffusion index changes following chemoradiotherapy: a prospective study using tract-based spatial statistics. *Plus One*. 2013; 8(3):e57768.
37. Hau C, Wu S, Chemaitilly W, et al. Predicting the probability of abnormal stimulated growth hormone response in children after radiotherapy for brain tumors. *International journal of radiation oncology, biology, physics*. 2012; 84(4):990–5.

Summary

We studied the hippocampal vascular dose-response as an early indicator of neurocognitive dysfunction in patients receiving partial brain radiotherapy. Radiation-induced hippocampal vascular changes were pronounced one month after completion of radiotherapy and were significantly correlated with memory function decline. Clinical factors of sex, age and edema impacted on the hippocampal vascular dose-response, resulting in a large effect on the older females.

**Fig. 1.**

Illustrations of dose effects interacting with Sex and Age on the mean K^{trans} changes one month post-RT. The mean K^{trans} changes are compared between males and females receiving greater or less than 19 Gy (A), between old and young (> or <50 years) patients receiving doses > and < 19 Gy (B), and between male and female and old and young patients receiving high and low doses (C). The dose effect was more pronounced in older females. The error bars represent Standard Error of Mean.

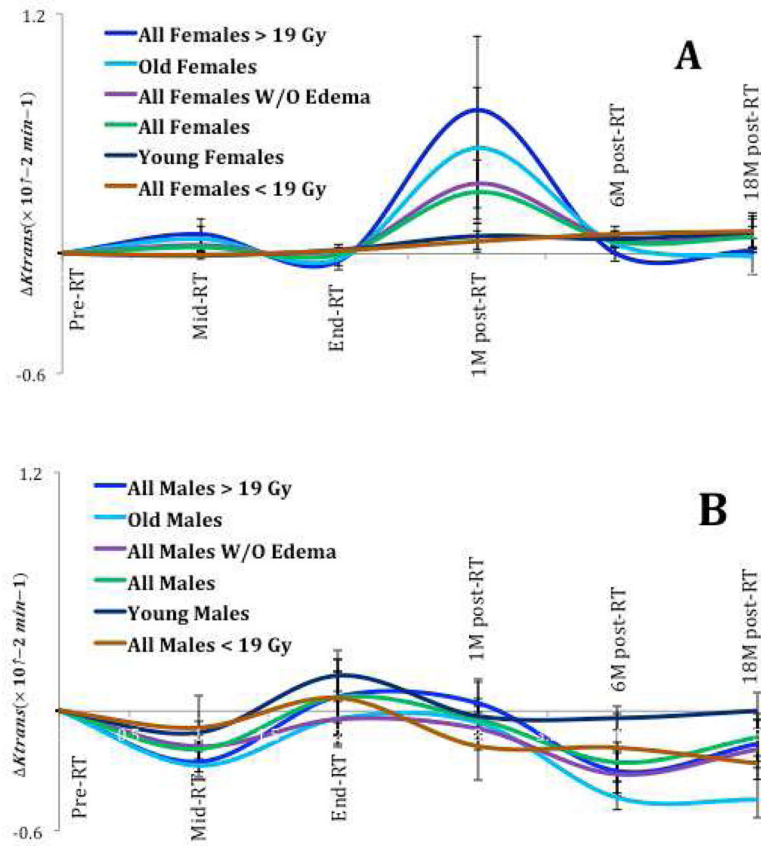


Fig 2.

The radiation-induced time profile changes in the mean K^{trans} of female (A) and male (B) hippocampi. The horizontal axes represent the time points: Pre-RT, week 3 during (Mid)-RT, End-RT, 1-month post-RT, 6-month post-RT and 18-month post-RT. The error bar represents the standard error of mean.

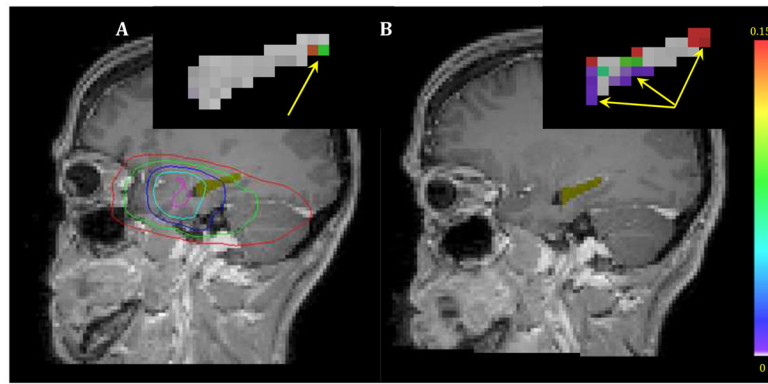


Fig. 3. Hippocampi (yellow color) and zoomed and color-coded K^{trans} maps overlaid on T1-weighted images pre-RT (A) and 1-month post-RT (B). The planned isodose curves, 5 (red), 10 (green), 20 (blue), 30 (cyan) and 40Gy (dark pink), are overlaid on the pre-RT image. Only a few voxels have K^{trans} values greater than zero pre-RT (colored voxels pointed by yellow arrows) (A). The BBB permeability increased 1-month post-radiation (colored voxels pointed by yellow arrows) (B).

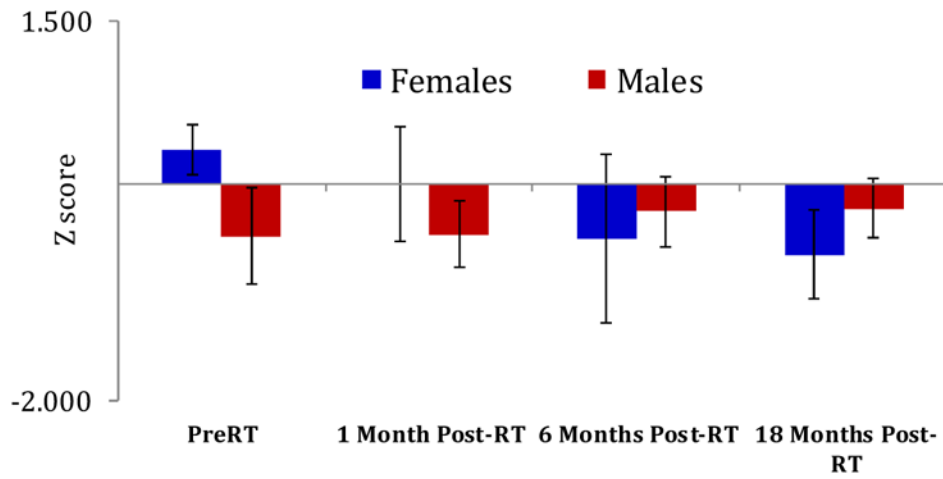


Fig. 4. The temporal changes in the delayed recall Z-scores of the revised Hopkins Verbal Learning Test from pre-RT to post-RT in males and females. The negative Z-score mean a negative deviation from the age- and education-matched standard Z-score of the normal population. Each bar represents standard error of mean.

Table 1

Patient characteristics

P#	A/S	Tumor Type	Tumor Location	Total dose/Ex	D _{mean} (range) LH ^{**}	D _{mean} (range) RH ^{**}
1*	43/M	Grade 2 Gemistocytic Astrocytoma	Right Temporal	59.4/1.8	15.2(11.7–24.4)	53.8(49.5–54.9)
2*	64/M	Sphenoid Wing Meningioma	Left Temporal, Petrous ridge	54/1.8	51.3(38.4–53.6)	39.7(18.9–49.1)
3	80/M	Pituitary Macroadenoma	Suprasellar	50.4/1.8	23.4(7.6–42.8)	28.2(8.8–44.7)
4*	47/M	Grade 2 mixed Oligoastrocytoma	Right Frontal, Temporal	59.4/1.8	31.6(22.5–44.4)	55.5(50.7–57.5)
5	38/M	Craniopharyngioma	Suprasellar	55.8/1.8	31.3(7.9–51.7)	31.5(4.1–51.6)
6*	38/M	Grade 2 diffuse Astrocytoma	Left Frontal, Temporal	54/1.8	51.4(50.8–52.2)	46.2(35.9–50.3)
7*	43/M	Grade 3 Anaplastic Supratentorial Ependymoma	Left Frontal	59.4/1.8	53.2(37.2–59.7)	24.3(18.3–37.1)
8	52/M	Pituitary Null-cell Adenoma	Suprasellar	50.4/1.8	26.5(1.9–46.5)	22.1(1.8–47.3)
9	51/M	Pituitary Macroadenoma	Suprasellar	50.4/1.8	12.3(1.05–43.6)	23.7(1.57–47.4)
10*	32/F	Grade 2 Glioma	Left Frontal, Temporal	54/1.8	55.2(49.7–59.3)	14.4(8.97–20.9)
11	70/M	Pituitary Macroadenoma	Suprasellar	50.4/1.8	23.2(2.08–44.7)	26.9(2.97–46.4)
12	62/M	Grade 2 Astrocytoma	Left Frontal	54/1.8	39.8(22.3–51.7)	29.4(15.4–39.7)
13	64/F	Pituitary Null-cell Adenoma	Suprasellar	50.4/1.8	11.9(1.1–36.7)	19.1(0.9–46.6)
14	57/F	Meningioma	Left Temporal, Parasellar	54/1.8	34.1(1.64–56)	23.9(1.45–53.7)
15*	31/F	Low grade Glioma	Left Frontal	54/1.8	54.3(45.4–56.3)	20.1(18.1–24.5)
16	60/M	Pituitary Null-cell Adenoma	Suprasellar	50.4/1.8	19.3(0.8–49.7)	11.7(0.7–46.8)
17	48/F	Pituitary Null-cell Adenoma	Suprasellar	50.4/1.8	4.4(0.9–29.6)	7(1–42)
18	48/M	Grade 2 diffuse Oligodendroglioma	Right Parietal	54/1.8	3.6(1.6–15.1)	23.6(9–53.2)
19	50/F	Pituitary Macroadenoma	Suprasellar	50.4/1.8	7.6(0.4–41.3)	9.4(0.5–40.1)
20	57/F	Meningioma	Left Parietal, Parasagittal	54/1.8	2(1.1–7)	4.2(1.4–11.4)
21	58/F	Grade 2 Gemistocytic Astrocytoma	Left Frontal	54/1.8	16.5(8.9–26.2)	6.1(3.1–8.5)
22	50/M	Pituitary Macroadenoma	Suprasellar	50.4/1.8	8.6(1.3–20.5)	12.2(2.7–30.9)
23	40/F	Meningioma	Left Occipital, Tentorial and Posterior Fossa	54/1.8	8.4(2.5–13.4)	3.4(2.1–4.5)
24	50/M	Meningioma	Right Cavemous sinus	54/1.8	8.2(1.14–21.1)	14.2(1.2–55.1)
25*	51/M	Grade 2 diffuse Astrocytoma	Left Temporal, Parietal	59.4/1.8	56.1(55.2–57.5)	16.8(15–18.8)
26	48/M	Pituitary Null-cell Adenoma	Suprasellar	54/1.8	17.5(1.2–49.3)	38.6(1.6–55.2)
27	32/F	Pituitary Craniopharyngioma	Suprasellar	55.8/1.8	11.3(0.9–42.3)	13.42(0.9–49.6)

Author Manuscript

Author Manuscript

Author Manuscript

Author Manuscript

Abbreviations: Pt # = Patient number; A/S = Age/Sex; M = Male; F = Female; D_{mean} = mean radiation dose in the hippocampus; LH = left hippocampus; RH = right hippocampus; Fx = fraction size.

* Hippocampus is affected by either tumor or edema.

** 2-Gy equivalent dose by the linear-quadratic equation with $\alpha/\beta = 2.5\text{Gy}$.